*Pak. J. Bot.*, 53(4): 1199-1208, 2021. DOI: http://dx.doi.org/10.30848/PJB2021-4(28)

# PLASTICITY IN STRUCTURAL AND FUNCTIONAL TRAITS ASSOCIATED WITH PHOTOSYNTHESIS IN *FIMBRISTYLIS COMPLANATA* (RETZ.) LINK. UNDER SALT STRESS

**MUHAMMAD KALEEM AND MANSOOR HAMEED***

*Department of Botany, University of Agriculture, Faisalabad 38040, Pakistan*
**Corresponding author's email: hameedmansoor@yahoo.com*

**Abstract**

*Fimbristylis complanata* (Retz.) Link. is a halophytic sedge and commonly found in salt-affected wetlands and salt marshes. This species is less explored, particularly no information available on salinity tolerance in the literature. In the present work, structural and functional modifications of photosynthesis in *F. complanata* were evaluated under salt stress. A complete randomized design with three replications and three salt regimes (0, 200 and 400 mM NaCl) were maintained throughout the experiment. Population SH collected from the highest saline habitat (ECe 49.28 dS $m^{-1}$) ranked as the highest tolerant, which showed an increase in biomass and chlorophyll pigments under salt stress. Modification in gas exchange parameters include decline in transpiration rate (*E*), while increase water use efficiency (WUE) and net $CO_2$ assimilation rate (P*n*), while structural modifications in SH population include increase in leaf succulence, cortical region thickness, bulliform thickness, aerenchyma formation, metaxylem and phloem area. Moderately saline population KM (ECe 29.56 dS $m^{-1}$) exhibited significant alterations, like *E* (transiently up to 200 mM NaCl) and maintence of P*n* up to 400 mM. This population altered leaf structural and epidermal traits related to photosynthetic efficiency. Least saline population LR (ECe 21.49 dS $m^{-1}$) accumulates high chlorophyll content, increased leaf succulence and secured higher abaxial stomatal density. Present results suggest that *F. complanata* could proficiently maintain photosynthesis by several structural and functional modifications.

**Key words:** Chlorophyll, Photosynthesis, Salinity tolerance, Structural modifications, Water use efficiency.

## Introduction

Soil salinization has become the key driving factor for land degradation all over the world (Ma *et al*., 2015). Salt-induced soil degradation is increasing rapidly and mainly caused due to the indiscriminate use of fertilizers and poor irrigation practices (Meena *et al*., 2019). Worldwide, saline soils account more than 831 Mha of the total area of the world (Amini *et al*., 2016), and inhabit 434 Mha of sodic and 397 Mha of saline soils (Anon., 2015). In Pakistan, salinization covers more than 7 Mha, as saline and sodic soils (Anon., 2017). Targeting salt-tolerant plant species to rehabilitate the salt effected soils is the basic necessity for the current era (Liang *et al.*, 2017). Salt tolerant plant species have a massive potential to rehabilitate and developed the salt-affected wetlands (Glenn *et al*., 2013).

Salinity has negative influence on the plant growth and productivity by altering the morpho-physiological traits, causing oxidative stress and ionic imbalance (Yamamoto *et al*., 2015; Ma *et al.*, 2017). Salinity induce osmotic stress, leading to disruption in photosynthesis (Hussain *et al*., 2019). High salinity lowers the rate of transpiration and cause stomatal closure which results in reduction of photosynthesis (Marsic *et al*., 2018). Salt stress causes more accumulation of $Na^+$ in chloroplast above the threshold by increasing the chlorosis and disrupting tissues (Flowers *et al.*, 2015). Salinity reduces the osmotic potential of mesophyll cells in leaves and curbs photosynthetic machinery, i.e., electron transport chain that results in a decline of photosynthesis (Chaves *et al*., 2009).

Halophytes mitigate salinity by osmotic adjustments, exclusion and homeostasis of $Na^+$, and attain tolerance in tissues by specific modifications (Kumari *et al*., 2019). These salt tolerant plants achieve modification in photosynthetic machinery over course of evolution. Halophytes thrive under saline extremities with no compromise and carry out efficient photosynthesis (Himabindu *et al*., 2016). These plants employ some structural and functional modifications to avoid from $Na^+$ and $Cl^-$ accumulation at a cellular level (Joshi *et al.*, 2015). Some obligate halophytes improve water use efficiency and net $CO_2$ assimilation rate (Rabhi *et al*., 2012). Salt tolerant plant deploy structural and functional changes in the ultrastructure of photosynthetic apparatus of leaf i.e. large mesophyll cells and broad lamina (Rozentsvet *et al.*, 2016), and improve activity of the antioxidant enzymes to reduce the level of reactive oxygen species (Guo *et al.*, 2021).

*Fimbristylis* genus of halophytic sedges and belongs to family Cyperaceae with a greater extent of salinity tolerance. *Fimbristylis complanata* is mostly found in salt marshes, salt-affected wetlands, and saline soils (Siwakoti & Tiwari 2007). Salinity tolerance of genus *Fimbristylis* is less explored, particularly little information on salt tolerance of *F. complanata* exists in the literature. The present research was aimed to explore the role of functional and structural traits in photosynthesis and modifications in *F. complanata* and elucidate degree of salinity tolerance, role of morphological, photosynthetic traits involved in photosynthesis. It is expected that differently adapted populations of *F. complanata* would respond differently to salinity stress under controlled conditions that might be because of their differential adaptation to a specific set of environments.

## Materials and Methods

**Collection sites:** Three populations of *Fimbristylis complanata* (Retz.) Link. were collected from differently salt-affected areas in the Punjab Province, Pakistan. These sites include Khewra Mines foothills (ECe 29.56 dS $m^{-1}$, coordinates: 32°38' 40" N, 73°00' 30" E, altitude 271 m a.s.l.), Lillah-Khewra foothills (ECe 21.49 dS $m^{-1}$, coordinates: 32°35' 29.30" N, 72°53' 33.42" E, altitude 206 m a.s.l.) and Sahianwala saltmarsh (ECe 49.28 dS $m^{-1}$, coordinates: 31°36' 08.45" N, 73° 14' 56.98" E, altitude 191 m a.s.l.).

**Plant growth conditions, establishment and layout:** The present research was carried out in the old Botanic Garden, University of Agriculture Faisalabad (coordinates: 31°25' 44" N, 73°04' 18" E, and altitude 186 m a.s.l.). Populations of *F. complanata* were established in plastic pots (each 45 cm in height and 30 cm in diameter) without any ameliorative treatment to accustom with the Faisalabad environment. Five rhizomes, containing plants at earlier growth stage (size 6 cm) were planted in each pot. Salt stress was applied after 30 days of plantation under varied salt (NaCl) levels (0, 100, 200 300 and 400 mM). Salt regimes were maintained gradually by adding 50 mM NaCl at an interval of 3 days to avert a sudden salt injury. After 60 days to salt imposition, the plants were carefully uprooted to assess fresh and dry weight and other physiological characteristics relating to functional modifications. Fresh leaf samples were kept at −20°C until the biochemical analysis was performed. After harvesting, the plants were oven-dried until the homogenous dry weight was achieved, and thereafter dry weight was measured on a digital balance (Model: FA2004B, YK Scientific Instrument, China).

## Plants analysis and measurements

**Soil physicochemical characteristics:** Rhizospheric soil samples were collected from each site to estimate soil physicochemical characteristics. Samples were taken half a meter away from the root area and at the depth of 15 and 25 cm depth. Collected soil samples were crushed into small pieces and oven-dried at 70°C until the soil was fully dried. Soil pH and ECe were recorded by using an ECe/pH meter (WTW series Ino LAB pH/Cond 720, USA). Soil $Na^+$ and $K^+$ were assessed by using a flame photometer (Jenway, PFP-7, UK) by extracting soil samples in deionized water and chloride ions ($Cl^-$) were determined by using a chloride meter (Model-926, Sherwood Scientific Limited Cambridge, UK). Concentration of $Ca^{2+}$ was estimated with atomic absorption spectrophotometer (Model, Analyst 3000: Perkin Elmer, NW, CT). Percentage of organic matters was assessed by following the method of Sims & Haby (1971). Soil moisture contents from fresh soil samples were measured immediately by a battery-operated digital balance. After measuring the fresh weight of soil, samples were oven-dried at 60°C until constant weight obtained. Dry weight of soil samples was taken by a digital weight balance. Moisture content was calculated by subtracting initial weight into final weight and divided by the initial weight of soil samples. Contents of $PO_4^{3-}$ was appraised by the following method of Kowalenko & Lowe (1973) and $NO_3^-$was determined according to the method of Yoshida *et al.*, (1976) by using a spectrophotometer.

**Morphological attributes:** To ascertain morphological attributes, five plants selected from each salt treatment, were detached from the soil and washed up with tap water. Plant height, numbers of leaves per plant were recorded. Leaf area was measured by using formula:

Length × width × correction factor 0.75.

The shoot fresh weight (SFW) was taken instantly after uprooting the plants.

**Gas exchange traits:** Net $CO_2$ assimilation rate (*A*) and transpiration rate (*E*) of fully expanded matured leaf were estimated through a portable infrared gas analyser system (LCA-4, ADC, Hoddesdon, England). Photosynthetic traits were assessed in the early morning under moderate light conditions. The IRGA apparatus was adjusted to molar airflow; 403.3 mmol $m^{-2}$ $s^{-1}$, vapour pressure; 6-9 bar, atmospheric pressure was 99.9 KPa; PAR, 1711 µmol $m^{-2}$ $s^{-1}$, level of $CO_2$ was 352 µmol $mol^{-1}$ with relative humidity 65% within the temperature of cuvette 25°C. Following equation was used to estimate the WUE.

WUE = A/E, *A* represents the net assimilation rate and *E* transpiration rate

**Photosynthetic pigments:** Plant leaves samples were homogenized in acetone at 0-4°C to assess chlorophyll *a*, *b* and carotenoids following the method of Arnon (1949). The homogenized plant extract was centrifuged at 10,000 rpm for 5 min and specific absorption was recorded at 480, 645, 663 nm wavelengths by using UV visible spectrophotometer (Hitachi-220, Japan).

**Anatomical characteristics:** For anatomical studies, the plant material was preserved in the FAA (formalin acetic alcohol) solution. The freehand sectioning technique was used for root, stem, and leaf transverse sections. The thickest adventitious root, tallest stem and largest leaf were selected for anatomical studies. After sectioning, a thin section was stained by following the double staining method in a series of varied alcohol concentrations (30, 50, 70, 90 and 100%). Two staining dyes, safranin and fast green, were used. The stained plant section was mounted on a glass slide by using Canada balsam and covered with a coverslip. Photographs of the prepared slides were taken by using a light microscope (Nikon 104, Japan). Anatomical features were measured by using an ocular micrometre calibrated with a stage micrometer.

## Statistical analysis

A complete randomized design (CRD) with three replicates and five treatments was used. To analyze, data were subjected to the Tukey pairwise comparison test between sites of different species followed by an analysis of variance (ANOVA) at the significance level ($p<0.05$) using the Minitab 19 software. Moreover, the data were subjected to the multivariate analysis (PCA), cluster analysis and correlation matrix by using an R statistical software (R Core Team, 2019) to assess the relationship between studied traits.

## Results

**Soil Physiochemical characteristics:** Soil organic matter and moisture content were the maximum in the least saline population collected from Lilla-Khewra foothills (LR). Soil ECe, $Na^+$, $K^+$, $Ca^{2+}$, $Mg^{2+}$, $Cl^-$, $PO_4{}^3$, and $NO3^-$were the maximum in Sahianwala (SH) population. Soil pH was the maximum in Lilla-Khewra foothills (LR) population (Table 1).

**Morphological traits:** Numbers of leaves and leaf area significantly ($p\leq0.05$) increased as salt levels increased within all populations. Maximum mean values for these traits were recorded in SH population (Table 2). Plant height significantly increased as the level of salinity increased in KM and as SH populations, while this trait was significantly reduced at 400 mM NaCl level in LR population (Table 2). Shoot fresh weight (SFW) and shoot dry weight (SDW) were the maximum at 200 mM salt level in LR and KM populations. The SFW and SDW were markedly increased up to 400 mM salt level in SH population of *F. complanata* (Table 2).

**Photosynthetic pigments:** Chlorophyll *a* and chlorophyll *b* significantly ($p\leq0.05$) increased up to 200 mM NaCl level, whereas these pigments reduced significantly at the highest salt level in LR and KM populations. The SH population was the only case where a consistent increase in Chl *a* and Chl *b* was observed with increasing salinity levels (Table 2). A marked increase in carotenoids was observed in LR and KM populations at 200 mM NaCl levels, while reduction occurred at 400 mM NaCl. Carotenoid content significantly increased in SH population by an increase in salt levels (Table 2).

**Photosynthetic traits:** Net $CO_2$ assimilation rate (*A*) was the maximum in LR and KM populations at 200 mM salt level, while *A* significantly increased in SH population with increasing saline levels (Table 2). Transpiration rate (*E*) in LR and KM population increased up to 200 mM NaCl, thereafter a significant reduction occurred at the highest salt level. A marked reduction in *E* was observed in SH population of *F. complanata* along salinity gradients (Table 2). Water use efficiency (WUE) significantly enhanced as the level of salinity increased in all populations (Table 2).

**Leaf anatomical characteristics:** Leaf lamina and midrib thicknesses showed a considerable increase in all populations with an increase in external salinity level, however, the maximum value for the traits was found in the SH population at 400 mM NaCl (Table 2, Fig. 1). All populations of *F. complanata* showed a substantial increase in cortical cell area up to the highest salt levels (Table 2). In the LR population, cortical cell area increased up to 200 mM salt level, however, the reduction was observed at 400 mM NaCl concentration. The KM and LR population showed a significant increase in cortical cell area up to the highest saline level (Table 2). Cortical thickness and bulliform thickness increased up to 200 mM salt level in LR and KM populations, while both of these traits significantly ($p\leq0.05$) increased in SH population along salinity gradients (Table 2). The KM and SH showed a significant increase in metaxylem area as salinity levels were increased, while this trait was the maximum in the LR population at 200 mM salt level (Table 2). Phloem area and vascular bundle area significantly increased in all populations of *F. complanata* along with elevated salt levels (Table 2). The LR and KM populations exhibited maximum vascular bundle numbers (VBN) at 200 mM, but higher salt level decreased this trait significantly ($p\leq0.05$) in both populations. The VBN increased gradually by an increase in salt levels in the SH population (Table 2). Aerenchymatous area increased gradually in all three populations as the levels of salinity increased. The mean value for aerenchymatous area was the maximum in SH population (Table 2).

**Leaf epidermis:** The abaxial stomatal area increased up to 200 mM NaCl, while reduction occurred thereafter in LR and KM populations. A significant gradual increase in abaxial stomatal area was observed in SH population as external NaCl levels increased (Table 2, Fig. 2). Adaxial stomatal area decreased as the level of salinity increase in LR and KM populations, while this trait showed an increase in SH population at 200 mM salt concentration (Table 2). Abaxial stomatal density in all three populations increased, while adaxial stomatal density reduced significantly with an increase in salt levels (Table 2).

**Multivariate analysis:** Principal component analysis (PCAs) revealed a significant effect of NaCl treatments on the morphological and physiological traits of *F. complanata* (Fig. 3a). The first and second PCAs explained 46.7% and 22.9% (69.6%) variability among the salt treatments and traits. The Chl *a*, SDW and E were the principal contributors to 200 mM salt level, and these traits secured a higher positive eigenvalue (+2.5) as shown in Fig. 3a. The major components of 400 mM NaCl were NLPP and LA with a significant reduction in negative eigenvalues (Fig. 3a).

Principal components analysis showed 70.6% and 12.5% (83.1%) variations among the anatomical traits of *F. complanata* (Fig. 3b). Major contributors to the absolute control 0 mM were only AdSD. Salt level 200 mM consisted only LTh as a principal component. However, the major contributor to 400 mM salt treatment was MXA, PhA, CCT, AbSD and MTh with positive eigenvalues (Fig. 3b).

**Table 1. Soil Physico-chemical characteristics of soil collected salt-affected sites (n = 3, means ± SE)**

| Characteristics | Lilla-Khewra foothills (LR) | Khewra mines foothills (KM) | Sahianwala (SH) |
|---|---|---|---|
| Habitat description | Seasonal inundation Lilla Khewra road side, least saline study site | Moderately salt-affected due to runoff water carrying salts from the Salt Range near Khewra Salt Mines | Hyper-saline salt marsh near Sahianwala, highly salt-affected site |
| Moisture contents (MC %) | 44.6 ± 0.21a | 21.9 ± 0.19c | 39.2 ± 0.40b |
| Organic matter (OM %) | 2.12 ± 0.12a | 1.36 ± 0.03b | 0.87 ± 0.01c |
| pH | 9.3 ± 0.33a | 6.9 ± 0.02c | 8.1 ± 0.11b |
| ECe (dS $m^{-1}$) | 21.49 ± 0.01c | 29.56 ± 0.10b | 49.28 ± 0.03a |
| $Na^+$ (mg $L^{-1}$) | 3675 ± 19.11b | 2714 ± 0.65c | 5344 ± 1.22a |
| $Mg^{2+}$ (mg $L^{-1}$) | 0.58 ± 0.01b | 0.45 ± 0.01c | 0.71 ± 0.03a |
| $K^+$ (mg $L^{-1}$) | 245 ± 0.48c | 414 ± 0.12a | 329 ± 0.58b |
| $Ca^{2+}$ (mg $L^{-1}$) | 131 ± 0.10b | 104 ± 0.15c | 174 ± 0.10a |
| $Cl^-$ (mg $L^{-1}$) | 1729 ± 3.45c | 3158 ± 6.51b | 4120 ± 3.75a |
| $PO_4^{3-}$ (mg $L^{-1}$) | 5.65 ± 0.04c | 7.15 ± 0.12b | 11.94 ± 0.13a |
| $NO_3^-$ (mg $L^{-1}$) | 4.51 ± 0.05b | 7.5 ± 0.11a | 3.5 ± 0.01c |

**Table 2. Morphological, photosynthetic traits and structural attributes of *Fimbristylis complanata* (Retz.) Link. collected from salt-affected areas (n = 3, means ± SE).**

| | Lilla-Khewra foothills (LR) | | | Khewra mines foothills (KM) | | | Sahianwala (SH) | | |
|---|---|---|---|---|---|---|---|---|---|
| **Traits** | **0 Mm** | **200 mM** | **400 mM** | **0 mM** | **200 mM** | **400 mM** | **0 mM** | **200 mM** | **400 mM** |
| | **Morphological traits** | | | | | | | | |
| NLPP | 15.00±0.50b | 16.67±0.76b | 18.67±0.76a | 16.00±0.50b | 17.67±0.29b | 19.20±0.22a | 15.33±0.29c | 18.33±0.29b | 27.00±0.50a |
| LA | 9.30±0.31c | 12.88±0.09b | 17.10±0.09a | 13.00±0.03c | 16.17±0.02b | 21.45±0.06a | 17.43±0.10c | 24.27±0.02b | 35.43±0.03a |
| PH | 72.67±3.06c | 115.00±3.12a | 92.00±6.08b | 60.00±4.36c | 74.00±1.50b | 88.33±5.01a | 63.50±6.22b | 78.00±6.06a | 44.53±3.38c |
| SFW | 2.57±0.18b | 3.77±0.08a | 2.80±0.09b | 4.53±0.16b | 5.63±0.16a | 3.67±0.10b | 2.53±0.28c | 3.60±0.20b | 5.05±0.09a |
| SDW | 1.23±0.10b | 1.97±0.03a | 1.10±0.18c | 1.06±0.06b | 1.37±0.10a | 0.77±0.06c | 0.93±0.08b | 0.95±0.07b | 1.29±0.01a |
| | **Chlorophyll pigments** | | | | | | | | |
| Chl *a* | 1.29±0.01b | 1.66±0.02a | 1.12±0.01c | 1.49±0.01b | 1.59±0.03a | 0.97±0.06c | 1.27±0.01c | 1.35±0.04b | 1.50±0.02a |
| Chl *b* | 0.63±0.01b | 1.18±0.03a | 0.61±0.03b | 0.68±0.02b | 1.32±0.08a | 0.52±0.01c | 0.58±0.01c | 1.22±0.03b | 1.52±0.01a |
| Caro. | 0.31±0.01b | 0.52±0.02a | 0.31±0.10b | 0.60±0.01a | 0.70±0.04a | 0.67±0.02a | 0.34±0.02c | 0.78±0.03b | 0.98±0.04a |
| | **Photosynthetic traits** | | | | | | | | |
| P*n* | 8.60±0.05b | 13.70±0.11a | 7.03±0.05b | 13.07±0.01a | 11.40±0.06b | 14.70±0.08a | 16.00±0.10b | 16.63±0.22b | 21.13±0.02a |
| *E* | 0.89±0.03b | 1.45±0.15a | 0.18±0.01c | 1.24±0.05b | 3.05±0.07a | 1.09±0.01c | 1.17±0.09a | 0.71±0.11b | 0.55±0.03c |
| *A/E* | 1.52±0.18c | 3.42±0.09a | 1.75±0.11b | 2.28±0.16c | 3.79±0.13b | 4.18±0.04a | 2.76±0.03c | 3.46±0.26b | 4.75±0.05a |
| | **Leaf anatomy** | | | | | | | | |
| MrTh | 231.70±25.4c | 285.14±10.2b | 471.95±20.4a | 244.01±20.7c | 340.42±42.5b | 367.65±20.3a | 388.67±28.4c | 513.08±11.9b | 734.54±10.2a |
| LTh | 201.53±6.24c | 223.6±26.83b | 314.0±4.05a | 186.84±26.5c | 234.53±10.5b | 429.34±3.50a | 323.31±8.50c | 596.17±31.1b | 790.63±6.24a |
| CCA | 1710.1±20.7c | 1753.6±27.7b | 1793.4±19.9a | 1406.9±75.4c | 1852.0±21.7b | 2172.0±50.0a | 2293.5±77.3c | 2699.6±12.8b | 3973.3±68.0a |
| CCT | 145.20±8.98b | 157.90±6.78a | 134.44±5.55c | 144.45±2.98b | 159.87±5.56a | 156.32±8.98a | 178.34±4.98b | 176.99±8.98b | 223.44±6.87a |
| BTh | 86.72±4.25c | 159.33±4.48a | 106.08±5.92b | 124.03±4.61a | 122.55±4.09a | 102.49±4.35b | 103.07±4.38c | 161.37±5.00b | 193.03±4.22a |
| CCTh | 16.08±1.33c | 38.13±4.72a | 27.23±1.43b | 22.03±2.14b | 43.57±4.72a | 19.88±2.10b | 34.04±3.12c | 46.30±2.36b | 76.30±2.36a |
| MXA | 594.4±15.98c | 952.2±37.6a | 839.1±23.54b | 442.3±20.86c | 1134.9±46.4b | 1685.8±23.9a | 773.6±56.7c | 874.5±18.36b | 1393.4±44.5a |
| PhA | 1838.2±5.29b | 1693.0±6.40c | 2782.7±1.62a | 4025.5±2.95c | 7150.1±3.48b | 8207.4±1.64a | 5563.1±7.52c | 7220.0±9.16b | 9723.6±6.87a |
| VBA | 9232.6±86.2c | 11270±91.4b | 11328±39.9a | 6749±72.6c | 9303.9±72.4b | 13229±53.4a | 11608±111.7c | 14793±65.7b | 23723±124.9a |
| VBN | 4.67±0.29b | 5.33±0.58a | 4.33±0.58b | 3.67±0.29c | 9.00±0.50a | 4.33±0.29b | 4.67±0.29c | 7.33±0.29b | 9.20±0.50a |
| ArcA | 3654.5±72.3c | 5882.1±87.8b | 6077.2±81.6a | 3908.3±26.4c | 5214.7±67.6b | 6667.7±78.2a | 4580.2±65.6c | 7794.6±98.8b | 10857±41.7a |
| | **Leaf epidermis** | | | | | | | | |
| AbSA | 3503.4±57.3c | 5090.6±20.4a | 3339.0±231b | 5011.4±14.1a | 4678.8±17.9b | 3282.1±60.9c | 2857.6±81.9c | 3470.8±32.5b | 3923.0±290a |
| AdSA | 6643±580.1a | 4964.8±47.1b | 3665.3±80.5c | 6713.0±319a | 3898±128.7b | 3288±43.7c | 1348±134.6b | 1672±320.4a | 1245.6±51.3c |
| AbSD | 40.67±1.26c | 51.33±0.76b | 62.67±2.08a | 34.67±1.26c | 48.67±1.04b | 68.00±1.80a | 39.33±1.26c | 64.67±1.04b | 100.67±2.52a |
| AdSD | 33.00±1.00a | 24.50±1.53b | 24.00±1.32b | 28.00±0.58a | 24.00±1.00b | 16.50±1.50c | 26.00±1.26a | 16.50±0.50b | 10.50±0.50c |

Means provided with error bars; different letter indicates significance ($p \leq 0.05$) between treatments

**NLPP**-numbers of leaves per plant**, LA**-leaf area, **PH**-plant height (cm), **SFW**-shoot dry weight (g/plant), **SDW**-shoot dry weight (g/plant), **Chl *a***-chlorophyll *a* (mg $g^{-1}$ FW), **Chl *b***- chlorophyll *b* (mg $g^{-1}$ FW), **P*n***- net $CO_2$ assimilation rate (µmol $m^{-2}s^{-1}$), ***E***- transpiration rate (mmol $m^{-2}s^{-1}$), **WUE**-water use efficiency (*A/E*), **MrTh**- mid rib thickness (µm), **LTh**- mid rib thickness (µm), **CCA**- cortical cell area (µm$^2$), **CCT**- cortical cell thickness, **BTh**- bulliform thickness, **CCTh**- chlorenchyma cell thickness (µm), **MXA**- metaxylem area (µm$^2$), **PhA**- phloem area (µm$^2$), **VBA**-vascular bundle area (µm$^2$), **VBN**- vascular bundle numbers, **AbSA**- abaxial stomatal area (µm$^2$), **AdSA**- adaxial stomatal area (µm$^2$), **AbSD**- abaxial stomatal density, **AdSD**- adaxial stomatal density

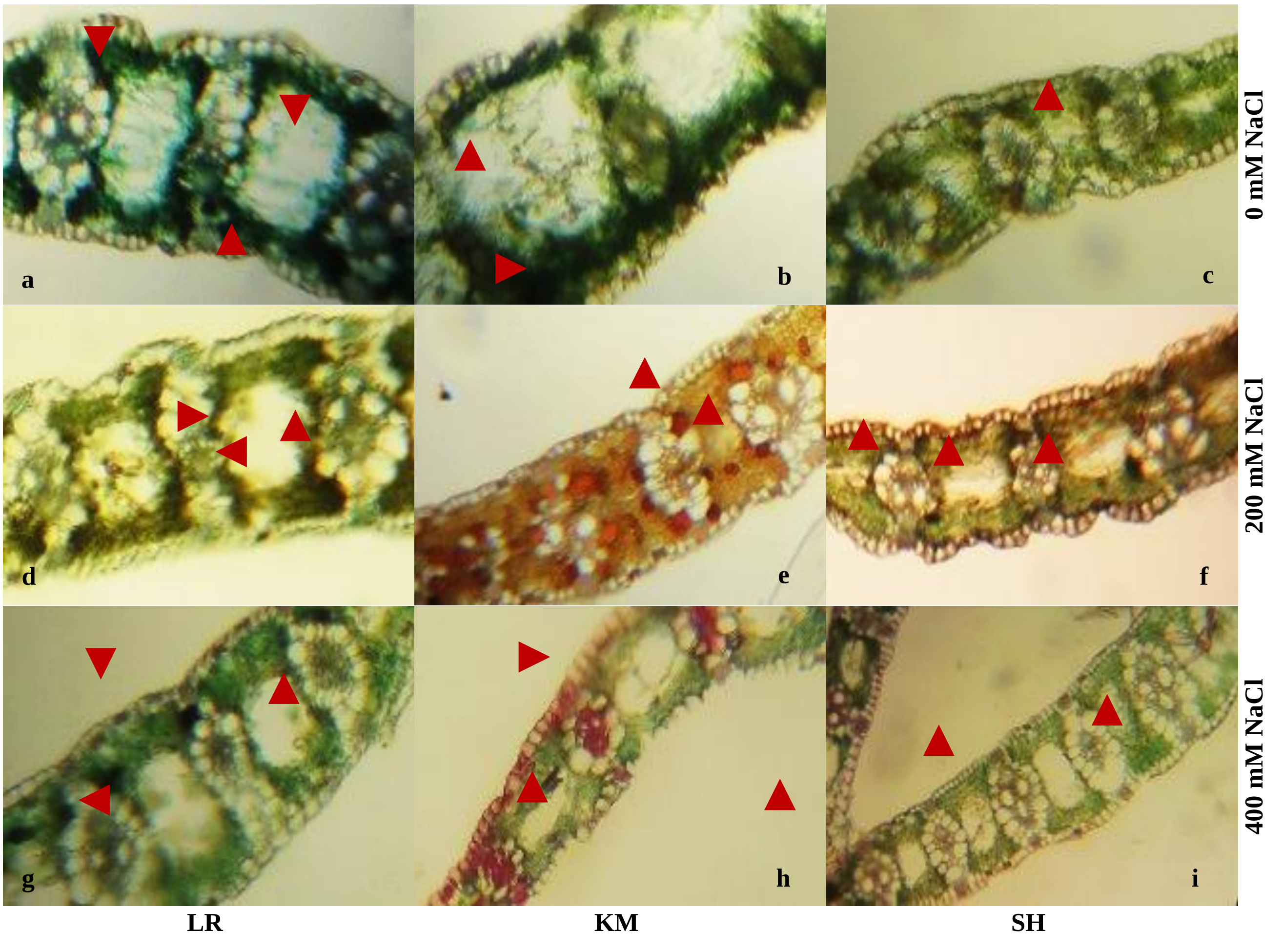


Fig. 1. Leaf transverse sections of *Fimbristylis complanata* collected from different salt affected habitats of Punjab, Pakistan [Lilla-Khewra foothills (LR); Khewra mines foothills (KM); Sahianwala (SH)].
**LR leaf anatomy: a. 0 mM:** well developed chlorenchyma, extensive sclerification beneath the epidermal cell layer, metaxylem cells exceptionally large **d. 200 mM** intensive sclerification around vascular bundles, large vascular bundles, Large lysigenous aerenchyma in cortical region **g. 400 mM** increased thickness of lamina and size of vascular bundles, large metaxylem. **KM leaf anatomy: b. 0 mM** Thick layer of sclerenchyma cells inside the epidermis, large air spaces present in cortical regions, **e. 200 mM** large epidermal cells and metaxylem cells. **h. 400 mM** increased thickness of lamina, large epidermal cells. **SH leaf anatomy: c. 0 mM** Extensive sclerification around vascular bundles, prominent and large chlorenchyma present **f. 200 mM** large air cavities present between vascular bundles **i. 400 mM** single layer of small epidermal cells, chlorenchyma relatively small, large vascular bundle present.

## Discussion

*Fimbristylis* is a genus of halophytic sedges that mostly inhabit saline wetlands and salt marshes (Zahoor *et al.*, 2012). *Fimbristylis complanata* mostly inhabits saline zones, swamps and salt marshes (Butt *et al.*, 2018). In the present study, populations of *F. complanata* collected from different salt-affected wetlands, showed varied response under different saline levels. Natural saline habitats vary in salinity level due to some key factors such as soil physicochemical characteristics, topography and microclimate (Bazihizina *et al*., 2009).

The salttolerant plants possess better growth under saline conditions by improving morphological traits (Yuan *et al.*, 2019). All populations of *F. complanata* showed variable response to salt stress regarding growth attributes. The highest tolerant population SH showed a consistent increase in most of the growth attributes which indicatesits hig degree of salt tolerance than the other populations. Similar findings have been reported by Muchate *et al.*, (2016) in a facultative halophytic *Sesuvium portulacastrum.* This resulted in an increase in fresh and dry biomass production of this population. Increased biomass under high salinities is an indication of high degree of salt tolerance as also been reported by Boestfleisch & Papenbrock (2017) and Atzori *et al.*, (2017) in halophytes. Halophytes do not exist in non-saline habitats because they need an optimal concentration of salt for better growth (Rozema & Schat, 2013).

Chlorophyll pigments are considered as a sensitive indicator of metabolic state under salt stress (Chattopadhyay *et al*., 2011). In present work, chlorophyll *a*, chl. *b* and carotenoids increased at lower salt level in least saline LR and moderately saline KM population, as also been reported by Amirjani (2011) and Sarabi *et al.*, (2017). The highest saline SH population contend higher amount of Chl *a*, *b* and carotenoids, increase in these pigments are in line with various studies reported a significant increase in photosynthetic pigments under saline conditions (Sghaier *et al.*, 2015; Rozentsvet *et al.*, 2017; Osman *et al*., 2020).

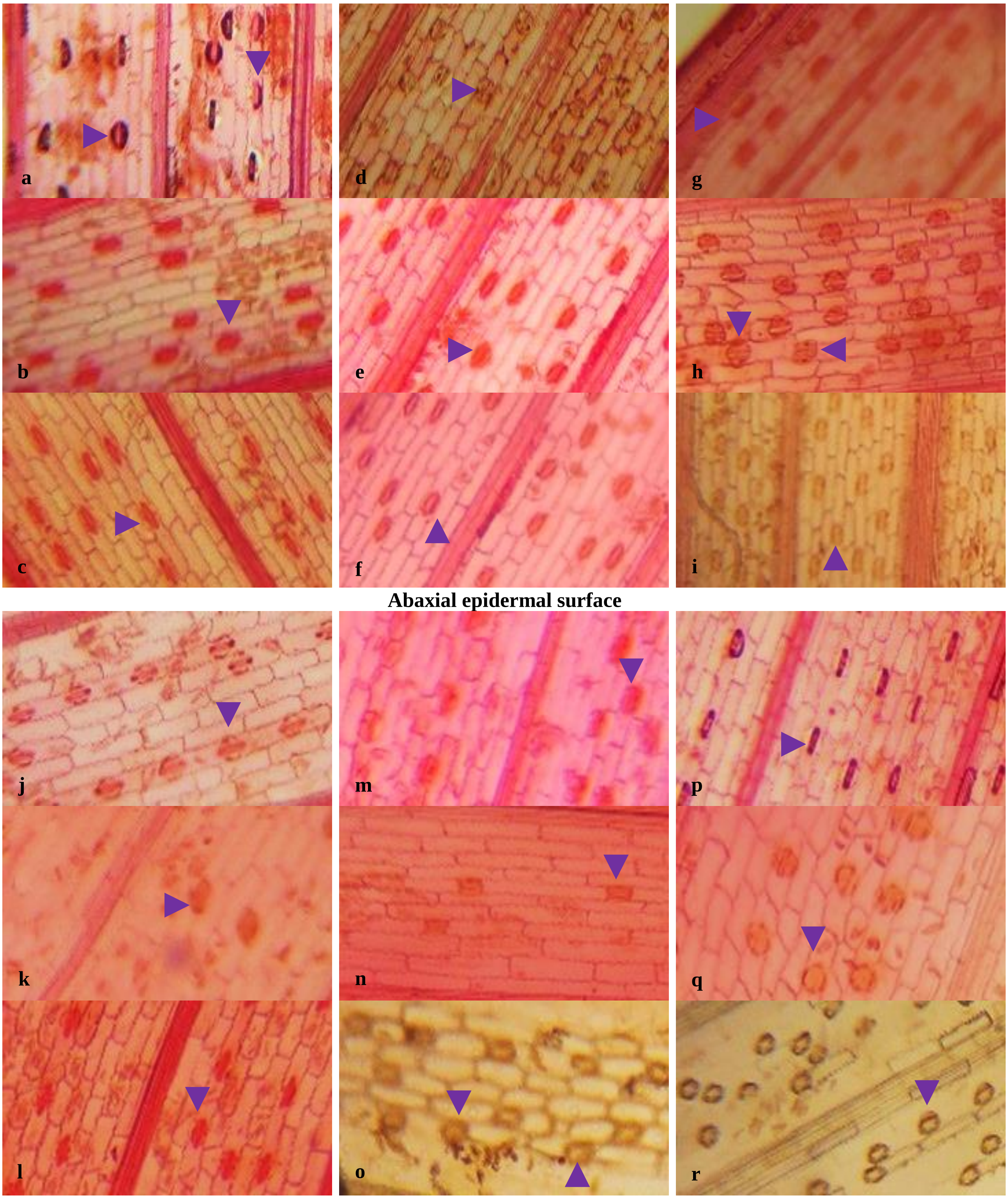


Fig. 2. Epidermal surface of *Fimbristylis complanata* collected from different salt affected habitats of Punjab, Pakistan [Lilla-Khewra foothills (LR); Khewra mines foothills (KM); Sahianwala (SH)].

**Abaxial epidermis of LR: a** 0 mM- Some stomata are elliptic, stomata small **b.** 200 mM- stomata large, nearly elliptic and elongated in stretched form **c.** 400 mM- stomata smaller in size, numerous, larger epidermal cells. **Abaxial epidermis of KM: d.** 0 mM-stomata small, round shape and arranged in three files between veins **e.** 200 mM-stomata enlarged, oval shape **f.** 400 mM – stomatal size reduce, nearly oval. Present after interval of two epidermal cells. **Abaxial epidermis of SH: g.** 0 mM-stomata arranged in a single linear file between major veins **h.** 200 mM-some stomata round, some ecliptic **i.** 400 mM- stomata area reduced, arranged between major veins.

**Adaxial epidermis of LR: j.** 0 mM- stomata large, twice as long, as broad **k.** 200 mM- less stomata with deformed shape. **l.** 400 mM- large elongated stomata. **Adaxial epidermis of KM: m.** 0 mM-stomata large, oval shape **n.** 200 mM- stomatal area reduced, stomata have spindle shape **o.** 400 mM – large circular stomata, epidermal cell area increased. **Adaxial epidermis of SH: p.** 0 mM-stomatal size much reduced, elongated in shape **q.** 200 mM- large stomata, circular in shape. **r.** 400 mM -stomatal area reduced, circular.

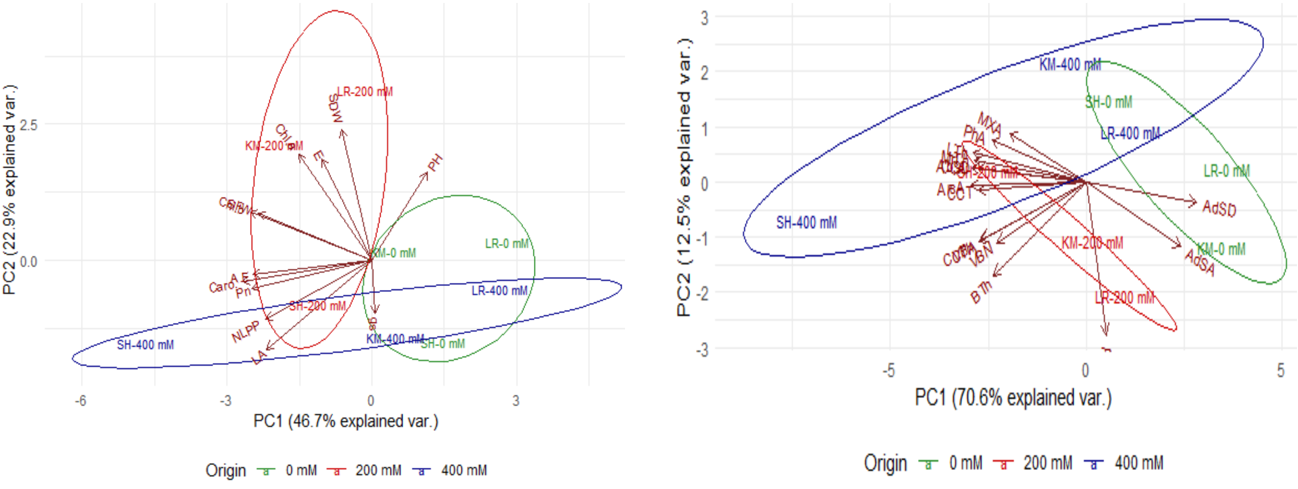


Fig. 3. PCA Biplot analysis for A) morphological and physiological traits B) leaf anatomical traits of *Fimbristylis complanata* collected from different salt effected sites (KM, Khewra mine foot hills; LR, Lillah-Khewra foothills; SH, Sahianwala) showing variation between traits.

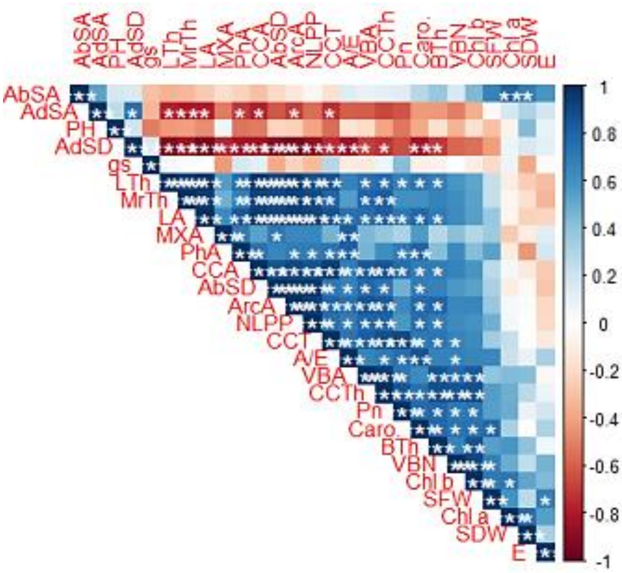


Fig. 4. Correlation among morphological, physiological, photosynthetic and anatomical traits.

**Figure legends: NLPP**-numbers of leaves per plant**, LA**-leaf area, **PH**-plant height (cm), **SFW**-shoot dry weight (g/plant), **SDW**-shoot dry weight (g/plant), **Chl *a***- chlorophyll *a* (mg $g^{-1}$ FW), **Chl *b***- chlorophyll *b* (mg $g^{-1}$ FW), **P*n***- net assimilation rate (µm $m^{-2}s^{-1}$), ***E***- transpiration rate (µm $m^{-2}s^{-1}$), **WUE**-water use efficiency (*A*/*E*), **MrTh**- mid rib thickness (µm), **LTh**-mid rib thickness (µm), **CCA**- cortical cell area (µ$m^2$), **CCT**-cortical cell thickness, **BTh**- bulliform thickness, **CCTh**-chlorenchyma cell thickness (µm), **MXA**- metaxylem area (µ$m^2$), **PhA**- phloem area (µ$m^2$), **VBA**- vascular bundle area (µ$m^2$), **VBN**- vascular bundle numbers, **AbSA**- abaxial stomatal area (µ$m^2$), **AdSA**- adaxial stomatal area (µ$m^2$), **AbSD**- abaxial stomatal density, **AdSD**- adaxial stomatal density.

Photosynthesis is considered an imperative biochemical process in which plants convert solar energy into chemical energy (Parihar *et al*., 2015). In the present study, high salt level resulted in an increase of photosynthetic rate (P*n*). Sengupta and Majumder (2009) also reported maintenance or even increase in P*n* in *Porteresia coarctata*. Increase in photosynthetic rate is strongly correlated with photosynthetic pigments and water use efficiency in *F. complanata*. Transpiration rate (*E*) in all populations of *F. complanata* reduced significantly, as reduction in *E* is a survival strategy to reduce water loss under salinity induced osmotic stress (Harris *et al.*, 2010). Populations of *F. complanata* showed an increasing trend in instantaneous water use efficiency (WUE) at higher salt regimes. Increase in WUE is associated with increased rate of photosynthesis in *F. complanata* populations. Previous literature support increase in WUE as observed in *Atriplex halimus* (Chen *et al*., 2019; Pérez-Romero *et al*., 2020).

Leaf structural modification is considered as an important feature of halophytic plants to circumvent with higher saline conditions (Parida *et al*., 2016). Modifications in leaf structure cause a change in gas exchange and increase net photosynthetic efficiency of plants (Paradiso *et al*., 2017). Leaf succulence in term of leaf thickness (midrib and lamina thickness) increased in all populations of *F. complanata* along the salinity gradients. This increase occurs due to a high proportion of palisade parenchyma tissues and these palisade parenchyma contain most of the chloroplast which is directly engaged in photosynthesis (Paradiso *et al*., 2017). Increase in leaf thickness enhances the water storage capacity (Naz *et al.*, 2016; Rayner *et al*., 2016). Leaf succulence is a reliable source to monitor leaf water status (Afzal *et al*., 2017). Cortical cell area and thickness generally increased with increase in salt levels, while increase in the cortical cell also increase leaf succulence and this directly confer salinity tolerance and results in greater photosynthesis due to large proportion of mesophyll in cortical region (Han *et al*., 2013). Bulliform cell thickness increased significantly in all populations of *F. complanata*, as bulliform cells roll the leaf (Xiang *et al.*, 2012), and reduce the loss of water and ensure the water conservation, which is an important commodity under salt-induced water stress (Hajihashemi *et al*., 2020). Leaf rolling under stress is convenient for better photosynthesis (Zhou *et al*., 2018). Chlorenchymatous thickness in a leaf of *F. complanata* population increased as salt levels increased. Chlorenchyma cell present in mesophyll cells fix atmospheric $CO_2$ and directly anticipate in the process of photosynthesis (Miszalski *et al*., 2017).

Metaxylem and phloem area increased in all populations of *F. complanata*, as large metaxylem and phloem vessels are positively correlated with efficient conduction of nutrients and water (Smith *et al*., 2013), as well as improved photosynthetic efficacy of plants (Akhtar *et al*., 2016). Salt tolerant plant species equipped with larger metaxylem vessels are vibrant for enhanced conduction of water (Naz *et al*., 2015; Naseer *et al*., 2017). Salt tolerant plants enhance phloem area for better distribution of photo-assimilates and it contributes to better growth (Lemoine *et al*., 2013). Vascular bundle area and number increased in an increase in all population of F. *complanata*, as this increase is considered as a more striking feature for better conduction of water and solutes (Batool & Hameed, 2013). Excessive numbers of vascular bundles in *Plantago media* increase photosynthesis (Miszalski *et al*., 2016).

Aerenchyma is a characteristic feature of plants colonizing waterlogged or saline waterlogged areas (Hameed *et al*., 2012; Al Hassan *et al*., 2015), which is responsible for gaseous exchange under anaerobic conditions (Evans 2004; Yamauchi *et al.*, 2013). Aerenchyma is a fast diffusion pathway for solutes that are involved in the bulk salt movement (Carter *et al.*, 2006; Lynch & Wojciechowski 2015; Watson *et al.*, 2015). Increase in aerenchymatous area, especially in the SH population may contribute to better translocation of water, nutrients, and salts for metabolic processes and ionic homeostasis throughout the plant body (Rahat *et al*., 2019). Large aerenchyma in seagrass enhances photosynthetic capability by storing excessive $CO_2$ concentration (Larkum *et al*., 2018).

A significant reduction was observed in the stomatal area in LR and KM populations under high salinity. Such reduction in the stomatal area is beneficial, especially when there is a limitation of water availability because the maintenance of cell turgidity requires less water and hence less energy (Naseer *et al*., 2017). The smaller stomatal size directly relates to faster stomatal response (Drake *et al.*, 2013), and even with high stomatal density, stomatal regulation will be easier. It also controls the transpiration rate under limited water availability (Doheny *et al*., 2012).

The present work demonstrates that halophyte *F. complanata* has greater amplitude for salinity tolerance by structural and functional modification. These modifications directly anticipate in better photosynthesis among all populations of *F. complanata*. The SH populations ranked as the highest tolerant by numerous modification in photosynthesis like higher biomass production, increase in chlorophyll pigments and WUE to ensure the cell water status and better photosynthesis and decrease rate of transpiration for water conservation. Population SH also showed structural modifications; increased leaf succulence due to high proportion mesophyll tissue for better photosynthesis, efficient bulliform cells for leaf rolling to prevent from water loss, large aerenchyma for gaseous exchange and efficient metaxylem for better conduction of water and phloem for the transport of photoassimilates. Moderately saline population KM also showed modifications in photosynthesis by lowering rate of transpiration low salinities. Population KM showed significant alteration in leaf structural and epidermis traits related to photosynthetic efficiency. Least saline population LR secured higher concentration of chlorophyll content, increase leaf succulence and higher abaxial stomatal density.

**Correlation matrix:** The traits studied under salt stress exhibited a significant correlation ($p<0.05$). The A/E, P*n* and Caro, SFW, and Chl *b*, MXA and PhA, LTh, BTh and MrTh were significantly and positively correlated. A negative correlation was assessed between *E* and PH, PHA and VBN, MXA and CCT (Fig. 4).

## Conclusion

In conclusion, present work validate that modifications in structural and functional greatly contribute to salinity tolerance and maintain photosynthetic efficiency. Population SH disclosed a greater performance and rated as high tolerant as compared to its counterparts. In future perspectives, these halophytic populations of *F. complanata* can use for the rehabilitation and reclamation of salt-affected soil and wetlands.

## Acknowledgement

The project is not funded by any organization.

### References

Afzal, A., S.W. Duiker and J.E. Watson. 2017. Leaf thickness to predict plant water status. *Biosyst. Eng.,* 156: 148-156.

Akhtar, N., M. Hameed and R. Ahmad. 2016. Structural and functional aspects of ionic relation in roots of *Typha domingensis* pers. ecotypes under salt stress. *Pak. J. Bot.,* 48: 2195-2203.

Al Hassan, M., G. Gohari, M. Boscaiu, O. Vicente and M.N. Grigore. 2015. Anatomical Modifications in two Juncus species under salt stress conditions. *Not. Bot. Hort. Agrobot. Cluj-Napoca.,* 43: 501-506.

Amini, S., H. Ghadiri, C. Chen and P. Marschner. 2016. Salt-affected soils, reclamation, carbon dynamics, and biochar: a review. *J. Soils Sed.,* 16: 939-953.

Amirjani, M.R. 2011. Effect of salinity stress on growth, sugar content, pigments and enzyme activity of rice. *Int. J. Bot.,* 7: 73-81.

Anonymous. 2015. Extent of Salt-Affected Soils. http://www.fao.org/soils-portal/soilmanagement/management-of-some-problem-soils/salt-affected soils/moreinformation-on-salt-affected-soils/en/.

Anonymous. 2017. FAO Agristat. http://www.fao.org.

Arnon, D.I. 1949. Copper enzymes in isolated chloroplasts. Polyphenoloxidase in *Beta vulgaris*. *Plant Physiol.,* 24: 1.

Atzori, G., A.C. De Vos, M. Van Rijsselberghe, P. Vignolini, J. Rozema, S. Mancuso and P.M. Van Bodegom. 2017. Effects of increased seawater salinity irrigation on growth and quality of the edible halophyte *Mesembryanthemum crystallinum* L. under field conditions. *Agric. Water Manag.,* 187: 37-46.

Batool, R. and M. Hameed. 2013. Root structural modifications in three *Schoenoplectus* (Reichenb.) Palla species for salt tolerance. *Pak. J. Bot.,* 45: 1969-1974.

Bazihizina, N., T.D. Colmer and E.G. Barrett-Lennard. 2009. Response to non-uniform salinity in the root zone of the halophyte *Atriplex nummularia*: growth, photosynthesis, water relations and tissue ion concentrations. *Ann. Bot.,* 104: 737-745.

Boestfleisch, C. and J. Papenbrock. 2017. Changes in secondary metabolites in the halophytic putative crop species *Crithmum maritimum* L., *Triglochin maritima* L. and *Halimione portulacoides* (L.) Aellen as reaction to mild salinity. *PLoS One,* 12: e0176303.

Butt, M.A., M. Zafar, M. Ahmad, S. Sultana, F. Ullah, G. Jan, A. Irfan and S.A.Z. Naqvi. 2018. Morpho-palynological study of Cyperaceae from wetlands of Azad Jammu and Kashmir using SEM and LM. *Microsc. Res. Tech.,* 81: 458-468.

Carter, J.L., T.D. Colmer and E.J. Veneklaas. 2006. Variable tolerance of wetland tree species to combined salinity and waterlogging is related to regulation of ion uptake and production of organic solutes. *New Phytol.,* 169: 123-134.

Chattopadhyay, A., P. Subba, A. Pandey, D. Bhushan, R. Kumar, A. Datta, S. Chakraborty and N. Chakraborty. 2011. Analysis of the grasspea proteome and identification of stress-responsive proteins upon exposure to high salinity, low temperature, and abscisic acid treatment. *Phytochem.,* 72: 1293-1307.

Chaves, M., J. Flexas and C. Pinheiro. 2009. Photosynthesis under drought and salt stress: regulation mechanisms from whole plant to cell. *Ann. Bot.,* 103: 551-560.

Chen, J., J. Zong, D. Li, Y. Chen, Y. Wang, H. Guo, J. Li, L. Li, A. Guo and J. Liu. 2019. Growth response and ion homeostasis in two bermudagrass (*Cynodon dactylon*) cultivars differing in salinity tolerance under salinity stress. *Soil Sci. Plant Nutr.,* 65: 419-429.

Doheny-Adams, T., L. Hunt, P.J. Franks, D.J. Beerling and J.E. Gray. 2012. Genetic manipulation of stomatal density influences stomatal size, plant growth and tolerance to restricted water supply across a growth carbon dioxide gradient. *Philosoph. Trans. Royal Soc. B: Biol. Sci.,* 367: 547-555.

Drake, P.L., R.H. Froend and P.J. Franks. 2013. Smaller, faster stomata: scaling of stomatal size, rate of response, and stomatal conductance. *J. Exp. Bot.,* 64: 495-505.

Evans, D.E. 2004. Aerenchyma formation. *New Phytol.,* 161: 35-49.

Flowers, T.J., R. Munns and T.D. Colmer. 2015. Sodium chloride toxicity and the cellular basis of salt tolerance in halophytes. *Ann. Bot.,* 115: 419-431.

Glenn, E.P., T. Anday, R. Chaturvedi, R. Martinez-Garcia, S. Pearlstein, D. Soliz, S.G. Nelson and R.S. Felger. 2013. Three halophytes for saline-water agriculture: An oilseed, a forage and a grain crop. *Environ. Exp. Bot.,* 92: 110-121.

Guo, H., S. Li, J. Ye, W. Min and Z. Hou. 2021. Ionomic and antioxidant system responses to $Na_2SO_4$ stress of two cotton cultivars differing in salt tolerance. *Pak. J. Bot.,* 53: 11-21.

Hajihashemi, S., S. Mbarki, M. Skalicky, F. Noedoost, M. Raeisi and M. Brestic. 2020. Effect of wastewater irrigation on photosynthesis, growth, and anatomical features of two wheat cultivars (*Triticum aestivum* L.). *Water,* 12: 607.

Hameed, M., T. Nawaz, M. Ashraf, A. Tufail, H. Kanwal, M.S.A. Ahmad and I. Ahmad. 2012. Leaf anatomical adaptations of some halophytic and xerophytic sedges of the Punjab. *Pak. J. Bot.,* 44: 159-164.

Han, Y., W. Wang, J. Sun, M. Ding, R. Zhao, S. Deng, F. Wang, Y. Hu, Y. Wang and Y. Lu. 2013. *Populus euphratica* XTH overexpression enhances salinity tolerance by the development of leaf succulence in transgenic tobacco plants. *J. Exp. Bot.,* 64: 4225-4238.

Harris, B.N., V.O. Sadras and M. Tester. 2010. A water-centred framework to assess the effects of salinity on the growth and yield of wheat and barley. *Plant Soil,* 336: 377-389.

Himabindu, Y., T. Chakradhar, M.C. Reddy, A. Kanygin, K.E. Redding and T. Chandrasekhar. 2016. Salt-tolerant genes from halophytes are potential key players of salt tolerance in glycophytes. *Environ. Exp. Bot.,* 124: 39-63.

Hussain, S., M. Shaukat, M. Ashraf, C. Zhu, Q. Jin and J. Zhang 2019. Salinity stress in arid and semi-arid climates: Effects and management in field crops. *Climate Change and Agriculture.* IntechOpen.

Joshi, R., V.R. Mangu, R. Bedre, L. Sanchez, W. Pilcher, H. Zandkarimi and N. Baisakh 2015. Salt adaptation mechanisms of halophytes: improvement of salt tolerance in crop plants. *n Elucidation of abiotic stress signaling in plants* Springer, New York, NY. 243-279.

Kowalenko, C. and L. Lowe. 1973. Determination of nitrates in soil extracts. *Soil Sci. Soci. Amer. J.,* 37: 660-660.

Kumari R, P. Kumar, D. Meghawal, V. Sharma and H. Kumar. 2019. Salt-Tolerance Mechanisms in Plants. In: Recent Trends in Tropical Plant Research, *AkiNik Publications, New Delhi.*

Larkum, A.W., M. Pernice, M. Schliep, P. Davey, M. Szabo, J.A. Raven, M. Lichtenberg, K.E. Brodersen and P.J. Ralph. 2018. Photosynthesis and metabolism of seagrasses. . In: *Seagrasses of Australia (pp. 315-342). Springer, Cham.*

Lemoine, R., S. La Camera, R. Atanassova, F. Dédaldéchamp, T. Allario, N. Pourtau, J.-L. Bonnemain, M. Laloi, P. Coutos-Thévenot and L. Maurousset. 2013. Source-to-sink transport of sugar and regulation by environmental factors. *Front. Plant Sci.,* 4: 272.

Liang, L., W. Liu, Y. Sun, X. Huo, S. Li and Q. Zhou. 2017. Phytoremediation of heavy metal contaminated saline soils using halophytes: current progress and future perspectives. *Environ. Rev.,* 25: 269-281.

Lynch, J.P. and T. Wojciechowski. 2015. Opportunities and challenges in the subsoil: pathways to deeper rooted crops. *J. Exp. Bot.,* 66: 2199-2210.

Ma, H., H. Yang, X. Lü, Y. Pan, H. Wu, Z. Liang and M.K. Ooi. 2015. Does high pH give a reliable assessment of the effect of alkaline soil on seed germination? A case study with *Leymus chinensis* (Poaceae). *Plant Soil,* 394: 35-43.

Ma, X., J. Zheng, X. Zhang, Q. Hu and R. Qian. 2017. Salicylic acid alleviates the adverse effects of salt stress on *Dianthus superbus* (Caryophyllaceae) by activating photosynthesis, protecting morphological structure, and enhancing the antioxidant system. *Front. Plant Sci.,* 8: 600.

Marsic, N.K., D. Vodnik, M. Mikulic-Petkovsek, R. Veberic and H. Sircelj. 2018. Photosynthetic traits of plants and the biochemical profile of tomato fruits are influenced by grafting, salinity stress, and growing season. *J. Agric. Food Chem.,* 66: 5439-5450.

Meena, M.D., R.K. Yadav, B. Narjary, G. Yadav, H. Jat, P. Sheoran, M.K. Meena, R. Antil, B. Meena and H. Singh. 2019. Municipal solid waste (MSW): Strategies to improve salt affected soil sustainability: A review. *Waste Manag.,* 84: 38-53.

Miszalski, Z., A. Kornaś and E. Kuźniak 2017. Photosynthesis-related functions of vasculature-associated chlorenchymatous cells. *Progress in Botany Vol. 79.* Springer.

Miszalski, Z., A. Skoczowski, E. Silina, O. Dymova, T. Golovko, A. Kornas and K. Strzalka. 2016. Photosynthetic activity of vascular bundles in *Plantago media* leaves. *J. Plant Physiol.,* 204: 36-43.

Muchate, N.S., G.C. Nikalje, N.S. Rajurkar, P. Suprasanna and T.D. Nikam. 2016. Plant salt stress: adaptive responses, tolerance mechanism and bioengineering for salt tolerance. *Bot. Rev.,* 82: 371-406.

Naseer, M., M. Hameed, A. Zahoor, F. Ahmad, S. Fatima, M.S.A. Ahmad, K.S. Ahmad and M. Iftikhar. 2017. Photosynthetic response in buttonwood (*Conocarpus erectus* L.) to salt stress. *Pak. J. Bot.,* 49: 847-856.

Naz, N., R. Batool, S. Fatima, M. Hameed, M. Ashraf, F. Ahmad and M.S.A. Ahmad. 2015. Adaptive components of tolerance to salinity in a saline desert grass *Lasiurus scindicus* Henrard. *Ecol. Res.* 30: 429-438.

Naz, N., S. Fatima, M. Hameed, M. Naseer, R. Batool, M. Ashraf, F. Ahmad, M.S.A. Ahmad, A. Zahoor and K.S. Ahmad. 2016. Adaptations for salinity tolerance in *Sporobolus ioclados* (Nees ex Trin.) Nees from saline desert. *Flora,* 223: 46-55.

Osman, M.S., A.A. Badawy, A.I. Osman and A.A.H.A. Latef. 2020. Ameliorative impact of an extract of the halophyte *Arthrocnemum macrostachyum* on growth and biochemical parameters of soybean under salinity stress. *J. Plant Growth Reg.,* 1-12.

Paradiso, R., C. Arena, V. De Micco, M. Giordano, G. Aronne and S. De Pascale. 2017. Changes in leaf anatomical traits enhanced photosynthetic activity of soybean grown in hydroponics with plant growth-promoting microorganisms. *Front. Plant Sci.,* 8: 674.

Parida, A.K., S.K. Veerabathini, A. Kumari and P.K. Agarwal. 2016. Physiological, anatomical and metabolic implications of salt tolerance in the halophyte *Salvadora persica* under hydroponic culture condition. *Front. Plant Sci*., 7: 351.

Parihar, P., S. Singh, R. Singh, V.P. Singh and S.M. Prasad. 2015. Effect of salinity stress on plants and its tolerance strategies: a review. *Environ. Sci. Pollut. Res.,* 22: 4056-4075.

Pérez-Romero, J.A., E. Mateos-Naranjo, J. López-Jurado, S. Redondo-Gómez and J.M. Torres-Ruiz. 2020. Importance of physiological traits vulnerability in determine halophytes tolerance to salinity excess: a comparative assessment in *Atriplex halimus*. *Plants,* 9: 690.

Rabhi, M., A. Castagna, D. Remorini, C. Scattino, A. Smaoui, A. Ranieri and C. Abdelly. 2012. Photosynthetic responses to salinity in two obligate halophytes: *Sesuvium portulacastrum* and *Tecticornia indica*. *South Afric. J. Bot.,* 79: 39-47.

Rahat, Q.U.A., M. Hameed and M.S.A. Ahmad. 2019. Contribution of root structural and functional features towards salinity tolerance in *Diplachne fusca* (L.) P. Beauv. ex Roem. & Schult. subsp. fusca. subsp. fusca. *Pak. J. Bot.,* 51: 773-779.

Rayner, J.P., C. Farrell, K.J. Raynor, S.M. Murphy and N.S. Williams. 2016. Plant establishment on a green roof under extreme hot and dry conditions: The importance of leaf succulence in plant selection. *Urban Forest. Urban Green.,* 15: 6-14.

Rozema, J. and H. Schat. 2013. Salt tolerance of halophytes, research questions reviewed in the perspective of saline agriculture. *Environ. Exp. Bot.,* 92: 83-95.

Rozentsvet, O., E. Bogdanova, L. Ivanova, L. Ivanov, G. Tabalenkova, I. Zakhozhiy and V. Nesterov. 2016. Structural and functional organization of the photosynthetic apparatus in halophytes with different strategies of salt tolerance. *Photosynthetica,* 54: 405-413.

Rozentsvet, O., V. Nesterov and E. Bogdanova. 2017. Structural, physiological, and biochemical aspects of salinity tolerance of halophytes. *Russ. J. Plant Physiol.,* 64: 464-477.

Sarabi, B., S. Bolandnazar, N. Ghaderi and J. Ghashghaie. 2017. Genotypic differences in physiological and biochemical responses to salinity stress in melon (*Cucumis melo* L.) plants: prospects for selection of salt tolerant landraces. *Plant Physiol. Biochem.,* 119: 294-311.

Sengupta, S. and A.L. Majumder. 2009. Insight into the salt tolerance factors of a wild halophytic rice, *Porteresia coarctata*: a physiological and proteomic approach. *Planta,* 229: 911-929.

Sghaier, D.B., B. Duarte, I. Bankaji, I. Caçador and N. Sleimi. 2015. Growth, chlorophyll fluorescence and mineral nutrition in the halophyte *Tamarix gallica* cultivated in combined stress conditions: Arsenic and NaCl. *J. Photochem. Photobiol. B: Biol.,* 149: 204-214.

Sims, J.R. and V.A. Haby. 1971. Simplified colorimetric determination of soil organic matter. *Soil Sci.,* 112: 137-141.

Siwakoti, M. and S. Tiwari. 2007. Emerging needs of wetlands protection for the conservation of wild rice biodiversity in Nepal: A case study from Lumbini area. *Sci., World,* 5: 95-99.

Smith, M.S., J.D. Fridley, J. Yin and T.L. Bauerle. 2013. Contrasting xylem vessel constraints on hydraulic conductivity between native and non-native woody understory species. *Front. Plant Sci.,* 4: 486.

Watson, E.B., H.M. Andrews, A. Fischer, M. Cencer, L. Coiro, S. Kelley and C. Wigand. 2015. Growth and photosynthesis responses of two co-occurring marsh grasses to inundation and varied nutrients. *Botany,* 93: 671-683.

Xiang, J.J., G.H. Zhang, Q. Qian and H.W. Xue. 2012. Semi-rolled leaf1 encodes a putative glycosylphosphatidylinositol-anchored protein and modulates rice leaf rolling by regulating the formation of bulliform cells. *Plant Physiol.,* 159: 1488-1500.

Yamamoto, N., T. Takano, K. Tanaka, T. Ishige, S. Terashima, C. Endo, T. Kurusu, S. Yajima, K. Yano and Y. Tada. 2015. Comprehensive analysis of transcriptome response to salinity stress in the halophytic turf grass *Sporobolus virginicus*. *Front. Plant Sci*., 6: 241.

Yamauchi, T., S. Shimamura, M. Nakazono and T. Mochizuki. 2013. Aerenchyma formation in crop species: a review. *Field Crop. Res.,* 152: 8-16.

Yoshida, S., D.A. Forno and J.H. Cock. 1971. Laboratory manual for physiological studies of rice. *IRRI, Los Banos.*

Yuan, F., J. Guo, S. Shabala and B. Wang. 2019. Reproductive physiology of halophytes: current standing. *Front. Plant Sci.,* 9: 1954.

Zahoor, I., M.S.A. Ahmad, M. Hameed, T. Nawaz and A. Tarteel. 2012. Comparative salinity tolerance of *Fimbristylis dichotoma* (L.) Vahl and *Schoenoplectus juncoides* (Roxb.) Palla, the candidate sedges for rehabilitation of saline wetlands. *Pak. J. Bot.,* 44: 1-6.

Zhou, Y., D. Wang, T. Wu, Y. Yang, C. Liu, L. Yan, D. Tang, X. Zhao, Y. Zhu and J. Lin. 2018. LRRK1, a receptor-like cytoplasmic kinase, regulates leaf rolling through modulating bulliform cell development in rice. *Mol. Breed.,* 38: 48.

(Received for publication 22 August 2019)